THE PUBLISHING HOUSE
OF THE ROMANIAN ACADEMY

PROCEEDINGS OF THE ROMANIAN ACADEMY, Series A,
Swpecial Issue/2018, pp. 129–134

THE OPTIMAL SPACING BETWEEN DIAMOND-SHAPED TUBES COOLED BY FREE CONVECTION USING CONSTRUCTAL THEORY

Ahmed WAHEED[*], Ansam ADIL[**], Ali RAZZAQ[**]

[*] Al-Nahrain University, College of Engineering, Mechanical Engineering Department, Baghdad, Iraq
[**] Al-Nahrain University, College of Engineering, Mechanical Engineering Department, Baghdad, Iraq
Corresponding author: Ahmed WAHEED, E-mail: ahmedwah76@gmail.com

Abstract. The optimal spacing between diamond-shaped tubes cooled by free convection is studied numerically. A row of isothermal diamond-shaped tubes is installed in a fixed volume and the spacing between them is selected according to the constructal theory (Bejan's theory). In this theory, the spacing between the tubes is chosen such that the heat transfer density is maximized. A finite volume method is employed to solve the governing equations; SIMPLE algorithm with collocated grid is utilized for coupling between velocity and pressure. The range of Rayleigh number is ($10^3 \le Ra \le 10^5$), the range of the axis ratio of the tubes is ($0 \le e \le 0.5$), and the working fluid is air (Pr = 0.71). The results show that the optimal spacing decreases as Rayleigh number increases for all axis ratios, and the maximum density of heat transfer increases as the Raleigh number increases for all axis ratios and the highest value occurs at axis ratio (e = 0, flat plate) while the lowest value occurs at (e =0.5) (rhombic tube). The results also show that the optimal spacing is unchanged with the axis ratio at constant Rayleigh number.

Key words: Diamond Tubes, Constructal Theory, Free Convection.

1. INTRODUCTION

According to the constructal theory, the optimal spacing between a heat generating devices (plates, fins, cylinders, etc.) is defined as the spacing that provides easier access of heat flow from these devices to the coolant streams. The quest of easier heat flow motivates the designers to find the optimal spacing between parallel plates in forced, free, and mixed convection [1–3], the optimal spacing between circular cylinders in forced and free convection [4–5], and the optimal spacing between circular rotating cylinders in forced and free convection [6–7]. Free convection from square cylinders can be found in many devices, heat exchangers, and heat sinks with square pin fins [8]. Free convection from a single square cylinder was studied previously, for example [9–11]. The optimal spacing between horizontal square cylinders (rotated with 45^o, diamond-shaped) is not addressed yet. In this paper, evolutionary design is employed to find the optimal spacing between square cylinders installed in a fixed volume and cooled by free convection.

2. MATHEMATICAL MODEL

Consider a row of diamond-shaped tubes installed in a fixed volume per unit depth (h L) as shown in Fig. 1. The major axis of the diamond tube is (h/2) and the minor axis of the tube is (b). The axis ratio is defined as ($e = b/h$). The tubes are maintained at constant wall (hot) temperature of (T_w), the ambient fluid is maintained at constant temperature of (T_∞). The objective is to find the number of tubes or the tube – to – tube spacing (s) for different axis ratio (e) in order to maximize the heat transfer density. In this geometry there are two degrees of freedom, the first is the spacing (s) and the second is the axis ratio (e). The dimensionless governing equations for steady, laminar, and incompressible flow with Boussinesq approximation for the density in the buoyancy term can be written as [12]

$$\frac{\partial U}{\partial X}+\frac{\partial V}{\partial Y}=0\,, \tag{1}$$

$$U\frac{\partial U}{\partial X}+V\frac{\partial U}{\partial Y}=-\frac{\partial P}{\partial X}+\left(\frac{\mathrm{Pr}}{\mathrm{Ra}}\right)^{1/2}\left(\frac{\partial^2 U}{\partial X^2}+\frac{\partial^2 U}{\partial Y^2}\right), \tag{2}$$

$$U\frac{\partial V}{\partial X}+V\frac{\partial V}{\partial Y}=-\frac{\partial P}{\partial Y}+\left(\frac{\mathrm{Pr}}{\mathrm{Ra}}\right)^{1/2}\left(\frac{\partial^2 V}{\partial X^2}+\frac{\partial^2 V}{\partial Y^2}\right)+T\,, \tag{3}$$

$$U\frac{\partial T}{\partial X}+V\frac{\partial T}{\partial Y}=\frac{1}{\left(\mathrm{Ra}\,\mathrm{Pr}\right)^{1/2}}\left(\frac{\partial^2 T}{\partial X^2}+\frac{\partial^2 T}{\partial Y^2}\right). \tag{4}$$

The non-dimensionalised variables and groups used are

$$\left.\begin{aligned} &X=x/h, Y=y/h, U=uh/\alpha\left(\mathrm{Ra}\,\mathrm{Pr}\right)^{1/2}, V=vh/\alpha\left(\mathrm{Ra}\,\mathrm{Pr}\right)^{1/2}, P=ph^2/\alpha^2\rho\mathrm{Ra}\,\mathrm{Pr},\\ &T=t-T_\infty/T_W-T_\infty, \mathrm{Pr}=\nu/\alpha, \mathrm{Ra}=g\beta(T_W-T_\infty)h^3/\alpha\nu \end{aligned}\right\}. \tag{5}$$

Since the flow is symmetrical between the tubes, only half of the flow channel between two tubes can be used to find the spacing in the numerical solution. Half of the flow channel is shown in Fig. 2. The total dimensionless height of the channel is ($H_u + H + H_d$), the dimensionless upstream height (H_u) and the dimensionless downstream (H_d) are added to avoid the applying of incorrect velocity and temperature at the inlet and outlet of the channel. The flow and thermal dimensionless boundary conditions on the channel are shown in Fig. 2.

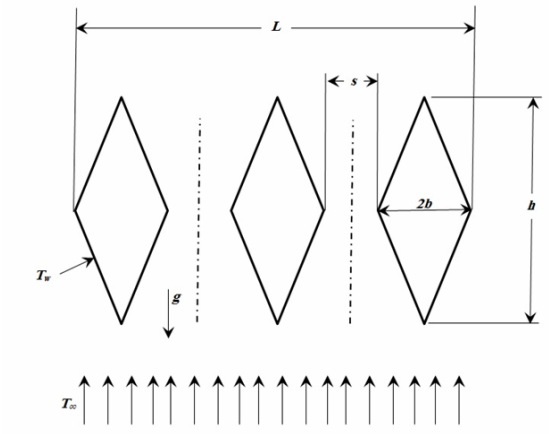

Fig. 1 – Physical geometry.

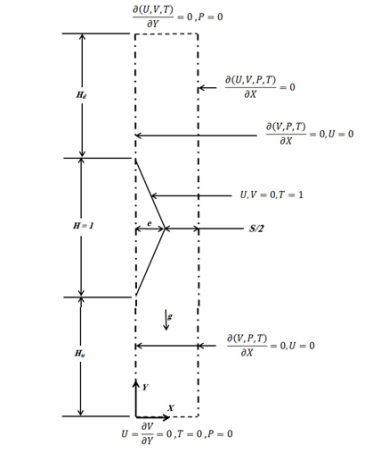

Fig. 2 – Dimensionless boundary conditions.

The right side of the downstream boundary condition is applied to permit fluid to enter the domain horizontally in order to avoid the vertical acceleration, which generated by chimney effects.

The spacing between the tubes is to be chosen such that the heat transfer density (objective function) is maximized. The heat transfer density is the heat transfer rate per unit volume and given as

$$q'''=\frac{q'}{(s+2b)h}, \tag{6}$$

where q' is the total heat transfer rate from one tube per unit width. The heat transfer density can be written in non-dimensional form as

$$Q=\frac{q'h^2}{k\left(T_w-T_\infty\right)(s+2b)h}=\frac{-\left(\int_0^h k\frac{\partial t}{\partial x}\mathrm{d}y\right)h}{k\left(T_w-T_\infty\right)(s+2b)h}=\frac{-\int_0^1\frac{\partial T}{\partial X}\mathrm{d}Y}{(S+2e)}\,. \tag{7}$$

3. NUMERICAL PROCEDURE, GRID INDEPENDENCE TEST, AND VALIDATION

A FORTRAN program is written to solve the algebraic equations, which obtained from the finite volume discretization. The general transport equation is firstly transformed to curvilinear coordinates and the convective term is discretized by hybrid scheme while the diffusion term is discretized by second order central scheme. For coupling between the pressure and velocity SIMPLE algorithm is employed. To prevent the oscillation in the pressure field the interpolation method of Rhie and Chow [13] is used. The convergence criterion of iteration is that the total imbalance in the source term in the pressure correction equation becomes less than 10^{-4}. Further computational details can be found in Rhie and Chow [13]. The grid independence test is performed for three grids for configuration at which (Ra = 10^4, e = 0.1, and S = 0.3). The grid independence test showed that the increasing of the grid size reduces the error percentage in the heat transfer density, and the minimum error is at (50×50) control volumes in the region ((e+S/2)×H). So this grid size is used and adopted in all results, gird independence test is illustrated in table (1). The upstream extension of (H_u = 0.5) and downstream extension of (H_d = 2) are used in the computational domain because it is observed that after double these extensions the variation in transfer density is less than 2.5%. The numerical results are validated by comparing the result of the optimal spacing with the result from the intersection of asymptotes of Bejan [14] for natural convection between vertical isothermal plates (e = 0) and (Ra =10^5). For this case, the optimal spacing in this study is (S_{opt} = 0.13) and the optimal spacing found in Bejan [14] was (S_{opt} = 0.129).

Table 1

Grid Independence Test for the Case (Ra = 10^4, e =0.1, and S =0.3)

Number of control volumes in the region ((e +S/2)xH)	Q	Error%
30×30	30.629	–
40×40	31.244	2
50×50	31.713	1.5

4. RESULTS AND DISSCUSION

The numerical results are presented in this section for, temperature contours, optimal spacing, and density of heat transfer for different values of tube axis ratio ($0 \le e \le 0.5$). The range of Rayleigh number is ($10^3 \le \mathrm{Ra} \le 10^5$) and the working fluid is air with (Pr = 0.71). Figure 3 shows the temperature contour as a function of the dimensionless spacing between the tubes (S) for (Ra = 10^3) and axis ratio (e = 0.1). For small spacing ($S \le 0.3$) the downstream region is occupied by hot fluid at temperature same as the wall temperature (red region), this is due to that the small spacing between the tubes prevents the cold air to flow downstream and the air there still hot (overworked fluid). As the spacing between the tubes increases ($S \ge 0.3$) the downstream temperature begins to decrease and become less than the wall temperature and this is clear from the appearance of the (orange, yellow and green) regions. At some spacing the thermal boundary layers from both sides are merged at the downstream region (the channel is fitted with the convective flow body), at this spacing the heat transfer density becomes maximum, and the spacing represents the optimal spacing, in this case (S_{opt} = 0.35). Further increasing in spacing between the tubes leads to a cold fluid region to appear in the downstream as seen in the blue region near the centerline (underworked fluid) for ($S \ge 1$), this large spacing permits the ambient (cold) fluid to flow downstream and leads to reduce the thermal conductance between the tubes and the surrounding fluid. Figure 4 illustrates the temperature contour for (Ra = 10^5) and (e = 0.1). The behavior of the temperature contour is similar to that of (Ra = 10^3) except that the spacing between the tubes here becomes smaller, note that at (Ra = 10^3) the hot (red) downstream region can be observed for ($S \le 0.3$)

while this region can be observed for ($S \leq 0.05$) at Ra = 10^5, the spacing decreases because the thermal boundary layer thickness decreases as Rayleigh number increases.

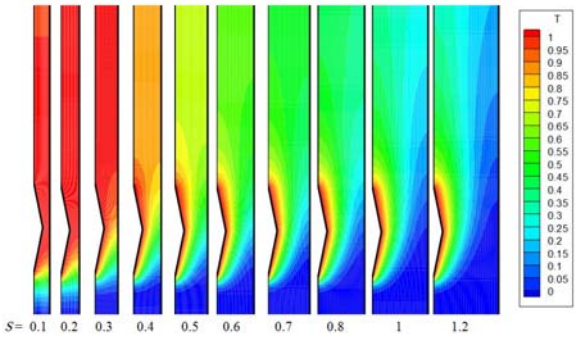

Fig. 3 – Temperature contour with various spacing between the tube for (Ra = 10^3, Pr = 0.7, and axis ratio e = 0.1).

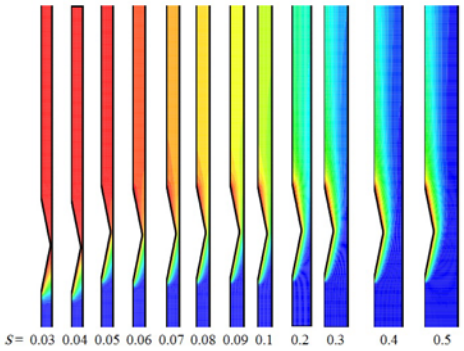

Fig. 4 – Temperature contour with various spacing between the tube for (Ra = 10^5, Pr = 0.7, and axis ratio e = 0.1).

As the axis ratio of the tube increases to (e = 0.5) (rhombic tube) for (Ra = 10^3), the thermal boundary layer on the upper surface becomes thicker than the thermal boundary layer on the upper surface of the tube of (e = 0.1) as shown in Fig. 5 for ($S \geq 0.3$). This thick thermal boundary layer reduces the heat transfer rate from the upper surface. For (Ra = 10^5) and as the axis ratio of the tube increases to (e = 0.5), a plume-like appears in temperature contours on the upper surface of the tube as shown in Fig. 6 for ($S \leq 0.06$). This plume-like region reduces the temperature gradient (*i.e.*, heat transfer rate) on the upper surface of the tube. Figure 7 shows the dimensionless heat transfer density as a function of the spacing at different Rayleigh numbers for (e = 0.1). This figure shows that there is an optimal spacing for each Rayleigh number. At this spacing the heat transfer density reaches its maximum value (tops of the curves). It is interesting to note that the optimal spacing decreases as Rayleigh number increases due to the decreasing of thermal boundary layer thickness.

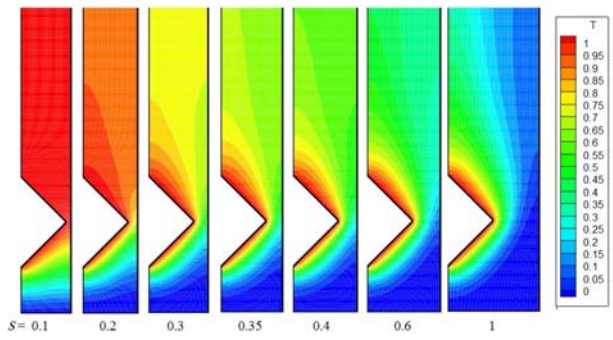

Fig. 5 – Temperature contour with various spacing between the tube for Ra = 10^3, Pr = 0.7, and axis ratio e = 0.5.

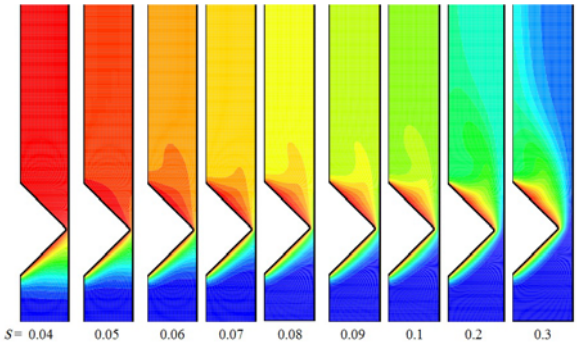

Fig. 6 – Temperature contour with various spacing between the tube for (Ra = 10^5, Pr = 0.7, and axis ratio e = 0.5.

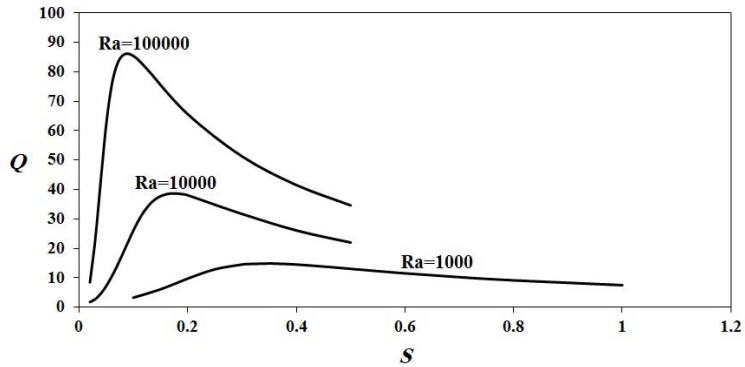

Fig. 7 – Heat transfer density with spacing at different Rayleigh numbers for axis ratio (e = 0.1).

Figure 8 shows the optimal spacing (S_{opt}) versus Rayleigh number for various axis ratios (e = 0, 0.1, 0.25, and 0.5), it is noted that the optimal spacing decreases as Rayleigh number increases for all values of (e). At constant Rayleigh number, the optimal spacing is almost unchanged for the range axis ratio ($0.1 \le e \le 0.5$). Since the optimal spacing is nearly unchanged with the axis ratio in the range ($0.1 \le e \le 0.5$), the number of tubes that installed in the same volume must be reduced as the axis ratio increases. Figure (9) shows the maximum heat transfer density versus Rayleigh number at various axis ratio (e), it can be noted that the maximum heat transfer density increases as Rayleigh number increases for all values of (e), the increasing of Rayleigh number leads to increase the buoyancy force and thus increase the maximum heat transfer density. It also can be seen that at each Rayleigh number the highest value of the maximum heat transfer density occurs at (e = 0, flat plate) and the lowest value occurs at (e = 0.5, rhombic tube). This can be explained as the geometry changes from flat plate to diamond-shaped tube, a plume-like is formed on the upper surface of the tube and the temperature gradient on the upper surface deceases and thus the maximum heat transfer density decreases.

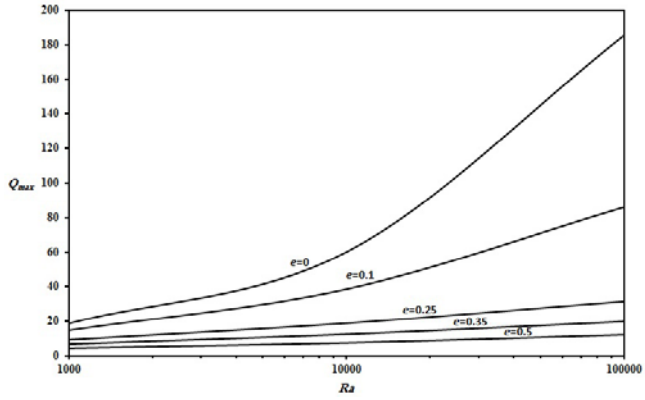

Fig. 8 – Maximum heat transfer density with Rayleigh number for different axis ratios.

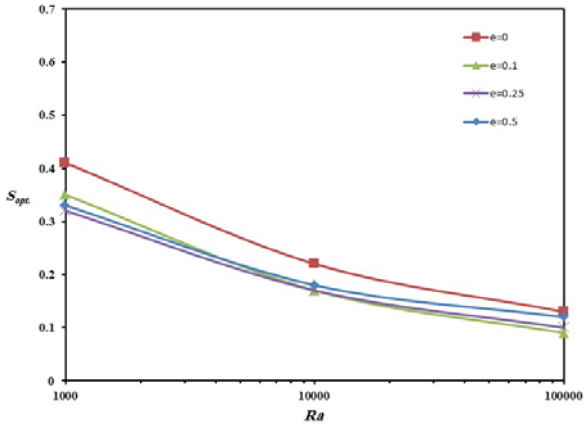

Fig. 9 – Maximum heat transfer density with Rayleigh number for different axis ratios.

5. CONCLUSIONS

The conclusions for optimal spacing between diamond-shaped tubes cooled by free convection can be summarized as:

1 – The optimal spacing decreases as Rayleigh number increases for all axis ratios.

2 – The maximum heat transfer increases as Rayleigh number increases for all axis ratios.

3 – The highest value of the maximum heat transfer density occurs at axis ratio (e = 0, flat plate) and lowest value occurs at axis ratio (e = 0.5, rhombic tube) for all Rayleigh numbers.

4 – The optimal spacing remains almost constant in the range ($0.1 \le e \le 0.5$) at constant Rayleigh number.

5 – The number of tubes installed in the same volume must be reduced as the axis ratio increases.

REFERENCES

1. BEJAN, A., SCIUBBA, E., *The optimal spacing for parallel plates cooled by forced convection*, International Journal of Heat and Mass Transfer **35**, pp. 3259–3264, 1992.

2. DA SILVA, A.K., BEJAN, A., LORENTE, S., *Maximal heat transfer density in vertical morphing channels with natural convection*, Numerical Heat Transfer Part A Applications **45**, pp. 135–152, 2004.

3. BELLO-OCHENDE, T., BEJAN, A., *Optimal spacings for mixed convection*, Journal of Heat Transfer, **126**, 6, pp. 956–962, 2004.

4 STANESCU, G., FOWLER, A.J., BEJAN, A., *The optimal spacing of cylinders in free-stream cross-flow forced convection*, International Journal of Heat and Mass Transfer, **39**, pp. 311–317, 1996.

5. BEJAN, A., FOWLER, J., STANESCU, G., *The optimal spacing between horizontal cylinders in a fixed volume cooled by natural convection*, Journal of Heat and Mass Transfer, **38**, pp. 2047–2055, 1995.

6. PAGE, L.G., BELLO-OCHENDE, T., MEYER, J.P., *Maximum heat transfer density rate enhancement from cylinders rotating in natural convection*, International Communications in Heat and Mass Transfer, **38**, pp. 1354–1359, 2011.

7. JOUCAVIEL, M., GOSSELIN, L., BELLO-OCHENDE, T., *Maximum heat transfer density with rotating cylinders aligned in cross-flow*, International Communications in Heat and Mass Transfer, **35**, pp. 557–564, 2008.
8. LEDEZMA, G., MOREGA, A.M., BEJAN, A. *Optimal spacing between pin fins with impinging flow*, **118**, pp. 570–577, 1996.
9. CHANG, K., CHOI, C., *Separated laminar natural convection above a horizontal isothermal square cylinder*, International Communications in Heat and Mass Transfer, **13**, pp. 201–208, 1986.
10. S. MAHMUD, D.P. KUMAR, N. HYDER, *Laminar natural convection around an isothermal square cylinder at different orientations*, International Communications in Heat and Mass Transfer, **29,** *7*, pp. 993–1003, 2002.
11. SASMAL, C., CHHABRA, R.P., *Effect of orientation on laminar natural convection from a heated square cylinder in power-law liquids*, International Journal of Thermal Sciences, **57**, pp. 112–125, 2012.
12. ZHANG Z., BEJAN A., LAGE J.L., *Natural convection in a vertical enclosure with internal permeable screen*, Journal of Heat Transfer, **113**, pp. 377–383, 1991.
13. RHIE, C. M., CHOW, W. L., *Numerical study of the turbulent flow past an airfoil with trailing edge separation*, AIAA Journal, **21**, pp. 1525–1532, 1983.
14. BEJAN A., *Convection Heat Transfer*, Wiley, New York, 1984.